ISSN 1063-7834, Physics of the Solid State, 2006, Vol. 48, No. 11, pp. 2046–2055. © Pleiades Publishing, Inc., 2006.
Original Russian Text © D.A. Balaev, S.I. Popkov, K.A. Shaĭkhutdinov, M.I. Petrov, 2006, published in Fizika Tverdogo Tela, 2006, Vol. 48, No. 11, pp. 1929–1937.

METALS AND SUPERCONDUCTORS

Investigation of the Josephson Coupling through a Magnetoactive Barrier (Ferrimagnet, Paramagnet) in $Y_{3/4}Lu_{1/4}Ba_2Cu_3O_7 + Y_3(Al_{1-x}Fe_x)_5O_{12}$ Composites

D. A. Balaev, S. I. Popkov, K. A. Shaĭkhutdinov, and M. I. Petrov

Kirensky Institute of Physics, Siberian Division, Russian Academy of Sciences, Akademgorodok, Krasnoyarsk, 660036 Russia
e-mail: smp@iph.krasn.ru

Received November 3, 2005; in final form, March 16, 2006

Abstract—The transport properties of two-phase composites consisting of a high-temperature superconductor and a nonsuperconducting component with magnetic ordering are analyzed. These composites are considered as a network of "superconductor–magnetoactive insulator–superconductor" weak links of the Josephson type. Substituted garnets $Y_3(Al_{1-x}Fe_x)_5O_{12}$ ($x = 0, \ldots, 1.0$) are used as a magnetoactive component. The composites under investigation contain 92.5 vol % $Y_{3/4}Lu_{1/4}Ba_2Cu_3O_7$ (the high-temperature superconductor) and 7.5 vol % $Y_3(Al_{1-x}Fe_x)_5O_{12}$ ($x = 0, \ldots, 1.0$). It is shown that an increase in the iron content in the $Y_3(Al_{1-x}Fe_x)_5O_{12}$ garnet leads to a reduction of the Josephson coupling strength: the temperature range in which the electrical resistance of the composites is equal to zero is reduced, and the critical current density at a temperature of 4.2 K decreases exponentially. For composites in which the iron content in the $Y_3(Al_{1-x}Fe_x)_5O_{12}$ garnet is higher than 0.1, the temperature dependence of the electrical resistance $R(T)$ at temperatures below the transition point T_C of high-temperature superconductor crystallites has a portion in the range T_m–T_C where the resistance $R(T)$ is independent of the transport current and the magnetic field strength. Below the temperature T_m, the dependences of the electrical resistance $R(T)$ of the composites are nonlinear functions of the current and involve a considerable contribution from magnetoresistance. This behavior is characteristic of a network of Josephson junctions. The temperature T_m decreases with an increase in the iron content in the $Y_3(Al_{1-x}Fe_x)_5O_{12}$ garnet. The appearance of the above feature in the temperature dependences of the electrical resistance $R(T)$ is interpreted as complete suppression of the Josephson coupling in the temperature range above T_m due to the interaction of supercurrent carrier pairs with magnetic moments of iron atoms in the dielectric barriers separating high-temperature superconductor grains.

PACS numbers: 74.72.Bk, 72.80.Tm, 77.84.Bw

DOI: 10.1134/S1063783406110023

1. INTRODUCTION

At present, composites with magnetoactive barriers separating superconductors (*S*) have been extensively investigated both theoretically [1–5] and experimentally [6–16]. Beginning with the pioneering works by Bulaevskii et al. [17, 18], who predicted remarkable effects accompanying the formation of π bonds between superconductors, special attention has been focused on Josephson junctions of the *S*–*F*–*S* type, where *F* stands for the material with magnetic ordering (ferromagnet or ferrimagnet). Moreover, particular interest has been expressed by researchers in the study of suppression of the superconducting properties of these Josephson junctions due to the scattering of Cooper pairs by magnetic moments in barriers [19–21]. In turn, this phenomenon can lead to complete suppression of the Josephson coupling [19, 20]. Furthermore, superconductor–insulator composites are characterized by a giant magnetoresistance effect [22], which can have practical applications.

For the most part, experimental works dealing with the investigation of *S*–*F*–S composites have been performed using low-temperature superconductors. Dilute ferromagnetic metals and alloys serve as *F* interlayers [6–12]. It should be noted that the preparation of structures based on high-temperature superconductors is a complex technological problem because of the high chemical reactivity of these materials and the necessity of producing very thin (several angstroms or several tens of angstroms) barriers between superconductors. It is clear that, in this case, the use of oxide materials in order to produce Josephson barriers is preferable [15, 16, 22].

The two-phase composites based on high-temperature superconductors can be considered as a network of weak links of the Josephson type [23–26]. It is worth noting that grain boundaries in high-temperature superconductor polycrystals are responsible for the Josephson coupling [27], whereas their role in composites is played by a nonsuperconducting component [23–26]. In our earlier papers [24–26], we demonstrated that the

transport characteristics of high-temperature superconductor composites, such as the temperature dependences of the electrical resistance $R(T)$ and the critical current density $j_C(T)$, as well as the current–voltage characteristics, reflect the main features of supercurrent carrier transfer through a single Josephson junction with an effective thickness. In this respect, investigation into the transport properties of composites containing nonsuperconducting components of different types is of considerable scientific interest and can provide deeper insight into the mechanism of current flow through Josephson junctions based on high-temperature superconductors. In our previous work [28], we analyzed the influence of magnetic scattering centers in the nonsuperconducting component (i.e., in barriers separating high-temperature superconductor crystallites) on the transport properties of high-temperature superconductor + CuNiO composites. Recent studies of high-temperature superconductor composites containing the $NiTiO_3$ paramagnetic [29] and $Y_3Fe_5O_{12}$ ferrimagnetic [26] compounds have revealed that, in the temperature range T_m–T_C ($T_m < T_C$, where T_C is the critical temperature of high-temperature superconductor crystallites), the electrical resistance is independent of the transport current and the magnetic field strength; i.e., the Josephson coupling is completely suppressed as a result of the interaction (scattering) of Cooper pairs and magnetic moments in barriers. By contrast, in the temperature range $T < T_m$, the current–voltage characteristics are nonlinear functions (the critical current exists at low temperatures) and the materials possess a high magnetoresistance [26, 29]. Investigation into the influence of the ferrimagnet–paramagnet–diamagnet transformations in the material of dielectric barriers separating high-temperature superconductor crystallites on the transport properties of the composites is a logical continuation of our earlier studies [26, 28, 29]. In the present work, we prepared composites containing a high-temperature superconductor and substituted garnets of the general formula $Y_{3/4}Lu_{1/4}Ba_2Cu_3O_7$ + $Y_3(Al_{1-x}Fe_x)_5O_{12}$ and examined their transport properties. The content of iron ions substituting for aluminum ions in the garnet lattice was chosen so that the mean distance between the iron ions (more precisely, the position of the maximum in the distribution function of the distances between the iron ions) was a multiple of the lattice constant of the garnet. Primary attention was concentrated on the change in the Josephson coupling strength and, as a consequence, in the behavior of the temperature dependences of the electrical resistance $R(T)$, the critical current density j_C, and the temperature T_m upon substitution of iron for aluminum in the aluminum garnet.

2. SAMPLE PREPARATION AND EXPERIMENTAL TECHNIQUE

Garnets of the general formula $Y_3(Al_{1-x}Fe_x)_5O_{12}$ at iron contents $x = 0$, 0.003, 0.025, 0.05, 0.10, 0.15, 0.30, 0.40, 0.60, 0.80, and 1.00 were synthesized from the Y_2O_3, Fe_3O_4, and $Al(OH)_3$ compounds at temperatures in the range 1000–1450°C for 320 h with seven intermediate grindings. It turned out that the x-ray powder diffraction patterns of the composites with intermediate iron contents $x = 0.6$ and 0.3 exhibit only the reflections attributed to the garnet structure. The lattice constant increases linearly from 11.9 Å at $x = 0$ to 12.3 Å at an iron content $x = 1.0$ upon substitution of iron for aluminum.

The polycrystalline high-temperature superconductor $Y_{3/4}Lu_{1/4}Ba_2Cu_3O_7$ was prepared using the standard ceramic technique. The composites were synthesized according to the rapid sintering procedure described in [24–26] under heat treatment at a temperature of 910°C for 2 min and then at a temperature of 350°C for 3 h [26]. The procedure used made it possible to prepare the two-phase composites and to minimize the possible chemical interaction of the yttrium high-temperature superconductor with the garnet. This was confirmed by the results of x-ray diffraction and magnetic measurements. By this means, we prepared composites containing 92.5 vol % $Y_{3/4}Lu_{1/4}Ba_2Cu_3O_7$ (the high-temperature superconductor) and 7.5 vol % $Y_3(Al_{1-x}Fe_x)_5O_{12}$. All the composites were synthesized in the same experimental cycle in order to exclude the influence of random factors on the physical properties. It what follows, the composite samples will be designated as $S + GR(\mathrm{Fe}, x)$, where x is the iron content in the $Y_3(Al_{1-x}Fe_x)_5O_{12}$ garnet.

The magnetic properties of the components were measured on a vibrating-sample magnetometer [30]. The temperature dependences of the electrical resistance $R(T)$ and the current–voltage characteristics were measured by the conventional four-point probe method. The samples were cut from the synthesized pellets in the form of parallelepipeds $1.5 \times 1.5 \times 8.0$ mm in size. The scatter in the electrical resistivity and the critical current density from sample to sample cut from the same pellet did not exceed 2%; i.e., it was determined by the accuracy in measuring the geometric parameters of the sample. The cross-sectional area and the distance between the potential contacts were identical for all samples. For this reason, the data on the electrical resistance and the transport current are given in units of Ω and mA, respectively. The critical current density j_C was determined from the initial portion of the current–voltage characteristic in accordance with a standard criterion of 1 μV/cm [31]. The magnetic field H was applied perpendicular to the direction of the transport current j through the sample.

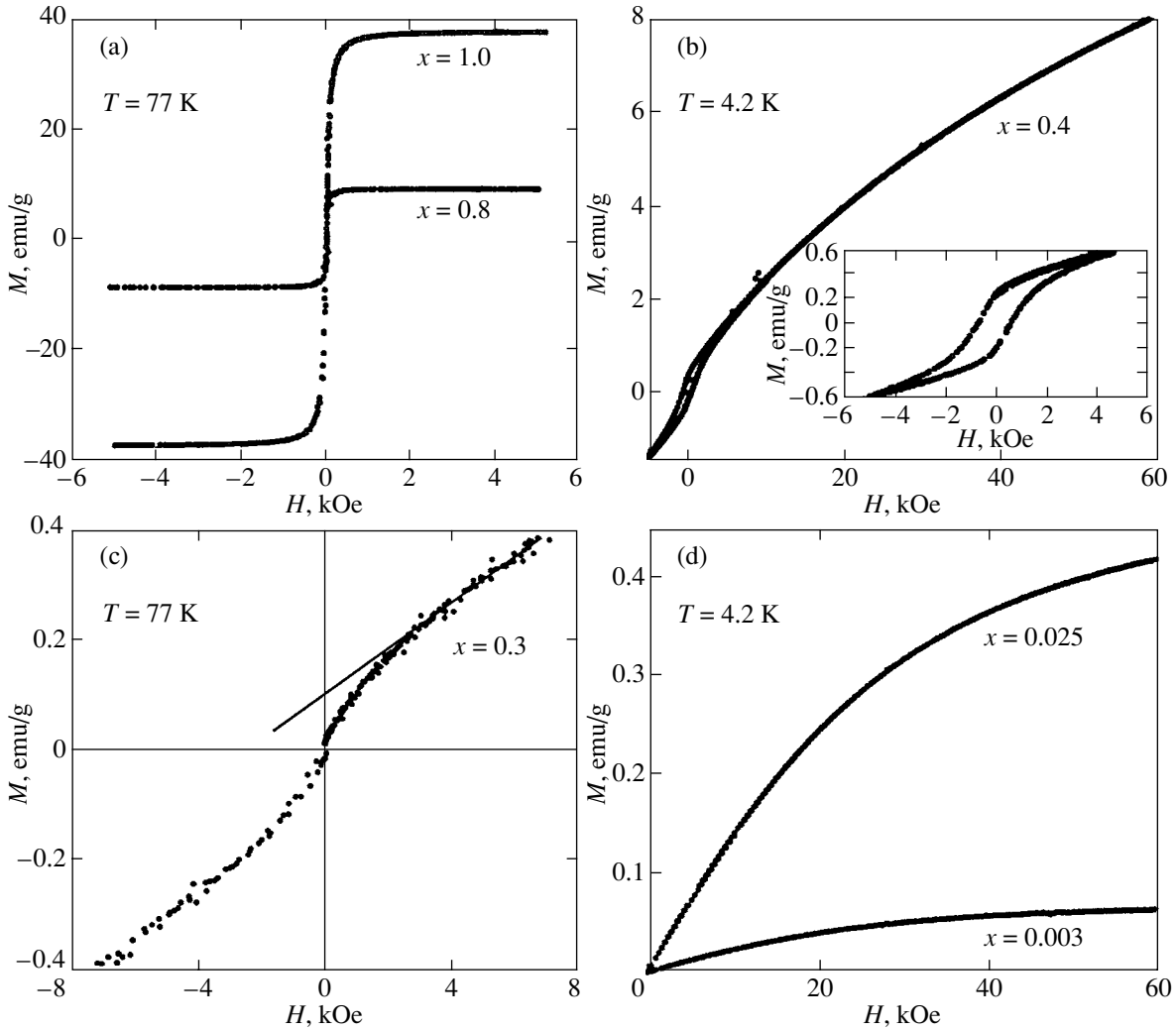

Fig. 1. Field dependences of the magnetization $M(H)$ for the $Y_3(Al_{1-x}Fe_x)_5O_{12}$ garnets with iron contents x = (a) 1.0, 0.8, (b) 0.4, (c) 0.3, and (d) 0.025, and 0.003.

3. MAGNETIC PROPERTIES OF THE $Y_3(Al_{1-x}Fe_x)_5O_{12}$ GARNETS

The $Y_3(Al_{1-x}Fe_x)_5O_{12}$ garnets were characterized using magnetic measurements. The field dependences of the magnetization $M(H)$ for a number of garnets are plotted in Fig. 1. The dependences $M(H)$ for the samples at iron contents $x = 1.0$ and 0.8 (Fig. 1a) are characteristic of ferrimagnets. The saturation magnetization and the magnetic moments per iron atom coincide with those obtained in [32–35]. Upon further substitution of iron for aluminum in the concentration range $0.1 < x < 0.8$, the dependences $M(H)$ correspond to a superposition of the ferrimagnetic and paramagnetic phases. It is worth noting that, since the samples have a single-phase composition according to the x-ray diffraction data, these magnetic phases coexist in the garnets. The typical dependences $M(H)$ in the above concentration range are depicted in Figs. 1b and 1c. The magnetization $M(H)$ increases drastically in weak fields and then smoothly reaches saturation in the field range 10–60 kOe. The remanent magnetization observed at $H = 0$ decreases with a decrease in the iron content x. The dependences for the samples at $x = 0.6$ and 0.4 exhibit a fairly wide hysteresis loop similar to that observed by Grasset et al. [34]. A decrease in the iron content x brings about an increase in the contribution from the paramagnetic phase and, accordingly, a decrease in the contribution from the ferrimagnetic phase. For the garnets at $x = 0.30$ and 0.15, the field dependences of the magnetization $M(H)$ involve an insignificant contribution from the ferrimagnetic phase. This can be clearly seen from Fig. 1c, which shows the field dependence of the magnetization $M(H)$ for the sample with $x = 0.3$ at 77 K (at this temperature, the paramagnetic contribution in magnetic fields up to ~10 kOe is linearly proportional to the magnetic field strength). It is known that, upon substitution of aluminum for iron, Al^{3+} ions predominantly occupy tetrahedral positions and the occupancy of octa-

hedral positions by Al^{3+} ions is considerably lower [32, 35, 36]. This leads to a faster decrease in the saturation magnetization as compared to the case where the octahedral and tetrahedral positions are occupied in proportion to their number in the garnet lattice [32, 36].

As was previously shown by Chen et al. [37] and Rotman [38] with the use of EPR spectroscopy, the garnets become paramagnets when the iron content is rather low ($x \ll 1$) and antiferromagnetic ordering is absent. The field dependences of the magnetization $M(H)$ for our samples at iron contents $x \le 0.1$ are typical of paramagnets (Fig. 1d) and can be adequately described by the Brillouin function. For the sample at $x = 0.003$, the saturation magnetization per iron atom is approximately equal to $\approx 5.2\mu_B$ (where μ_B is the Bohr magneton), which is close to the value for a free iron atom (~ 4.9–$5.4\mu_B$) [39].

The analysis of the temperature dependences of the magnetization $M(T)$ for the synthesized garnets has confirmed the above inferences. For the samples at $x \le 0.1$, the temperature dependences of the reciprocal of the magnetization are fitted fairly well by straight lines (Fig. 2). Although the extrapolation of the dependences $M^{-1}(T)$ to $M^{-1} = 0$ leads to an antiferromagnetic ordering temperature of ≈–30 K, this result is not surprising because the $Y_3Fe_5O_{12}$ initial compound is a ferrimagnet. It was also found that the Curie temperature determined from the dependence $M(T)$ for the sample at $x = 0.6$ is approximately equal to 213 K, which is close to the Curie temperatures obtained in [32, 34]. The Curie temperature for the sample at $x = 0.8$ is equal to 430 K [32].

Thus, the analysis of the results obtained from the magnetic measurements of the nonsuperconducting components of the composites has confirmed that the synthesized samples are solid solutions with a structure of the $Y_3(Al_{1-x}Fe_x)_5O_{12}$ garnet. The garnets at $x = 1.0$ and 0.8 are ferrimagnets. The samples at an iron content in the range $0.1 < x < 0.8$ contain a mixture of the ferrimagnetic and paramagnetic phases. The samples at $x \le 0.1$ are paramagnets.

4. TRANSPORT PROPERTIES OF THE $Y_{3/4}Lu_{1/4}Ba_2Cu_3O_7 + Y_3(Al_{1-x}Fe_x)_5O_{12}$ COMPOSITES

In our previous work [26], it was demonstrated that, at temperatures above the temperature T_C, the temperature dependences of the electrical resistance $R(T)$ for composites containing the $Y_3Al_5O_{12}$ and $Y_3Fe_5O_{12}$ garnets exhibit a quasi-semiconductor behavior. This circumstance is associated with the fact that the nonsuperconducting component is an insulator and that the transport current flows through the conducting component and tunnels through the nonconducting component. All the composites synthesized in the present work possess similar properties and are characterized by the ratio $R(100\ \text{K})/R(300\ \text{K}) \sim 1.5$.

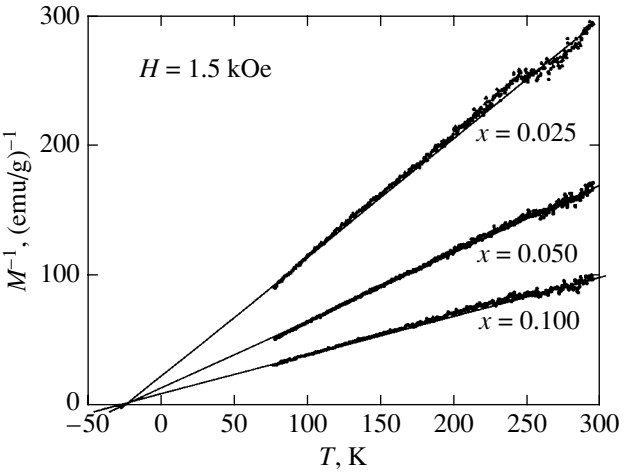

Fig. 2. Temperature dependences of the reciprocal of the magnetization $M^{-1}(T)$ for the $Y_3(Al_{1-x}Fe_x)_5O_{12}$ garnets with iron contents $x = 0.025$, 0.050, and 0.100.

The temperature dependences of the electrical resistance $R(T)$ for a number of composites in the temperature range 4.2–100 K are plotted in Fig. 3. For composites with the nonmagnetic dielectrics CuO [24], $MgTiO_3$ [29], and $Y_3Al_5O_{12}$ [26], the dependences $R(T)$ at temperatures below the temperature T_C are described in the framework of the Ambegaokar–Halperin model [40] accounting for thermal fluctuations in a Josephson junction. Let us analyze the temperature dependences of the electrical resistance $R(T)$. For all of the composites, the resistance R exhibits an abrupt jump at $T_C = 93.5$ K with a jump width of ≈2 K. This corresponds to a transition of high-temperature superconductor crystallites to the superconducting state. The next portion in the temperature dependence $R(T)$ below the temperature $T_{C1} = 91.5$ K reflects a transition of the network of Josephson junctions to the state with zero resistance. Previously, it was shown that this stage of the resistive transition of the composites is determined by the material (metal, insulator) forming the Josephson junction [24–26, 28, 29]. In Fig. 4, the superconducting transition is illustrated in detail by using the $S + GR$(Fe 0) and $S + GR$(Fe 0.4) samples as examples. For the $S + GR$(Fe 0) sample (Figs. 3h, 4a), the temperature range below the temperature T_C can be separated into two portions: the range T_{C0}–T_{C1} (where $T_{C1} \sim 91.5$ K and T_{C0} is the temperature above which the electrical resistance appears and the critical current disappears) and the range $T < T_{C0}$. In the range $T < T_{C0}$, the composites possess a critical current (see below) and an increase in the transport current and the application of a magnetic field lead to a shift in the temperature of disappearance of the electrical resistance toward the low-temperature range. In the range T_{C0}–T_{C1}, the current–voltage characteristics emerge from the origin of the coordinates ($j_C = 0$) and represent nonlinear functions of the current. This situation is illustrated in

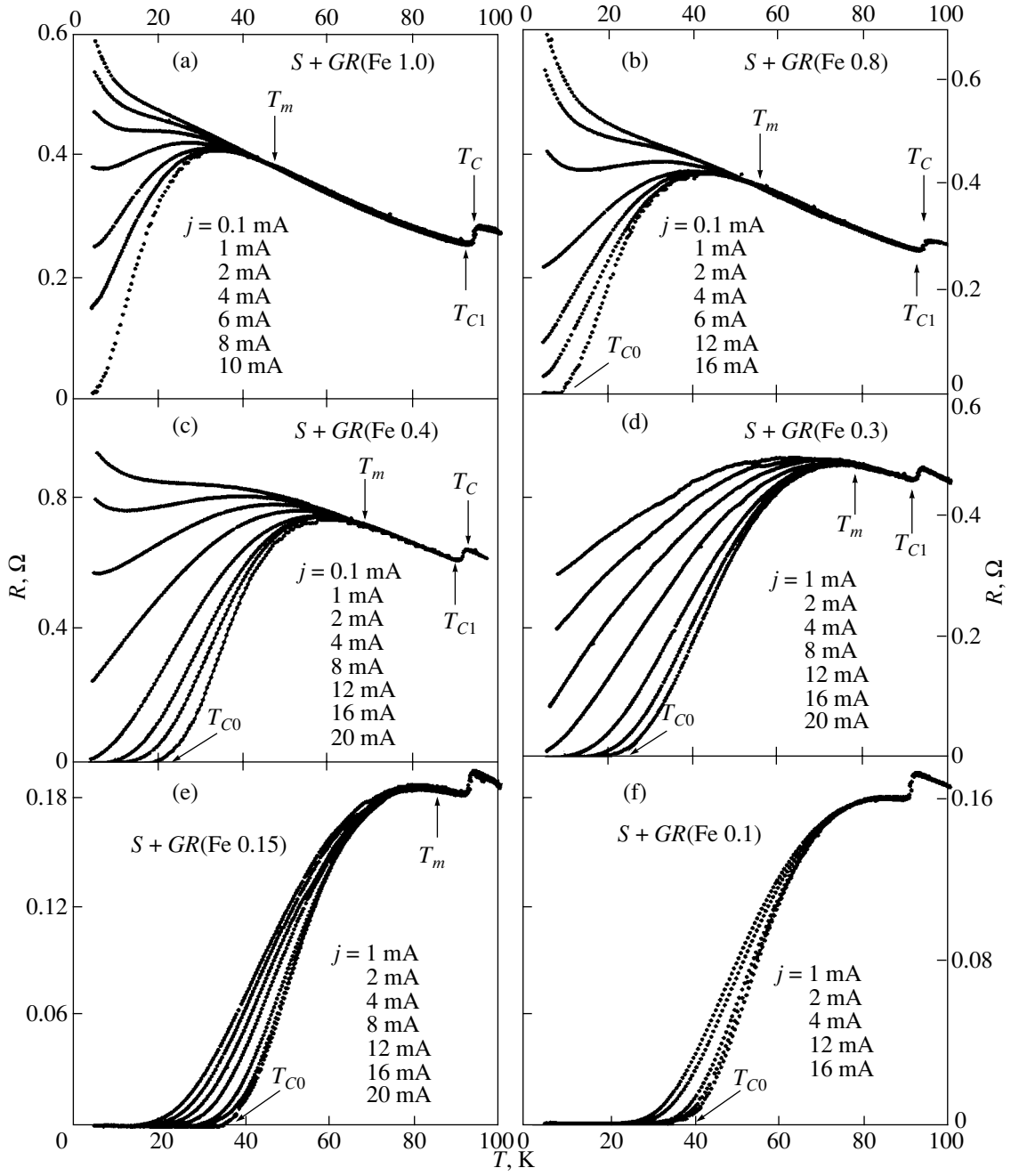

Fig. 3. Temperature dependences of the electrical resistance $R(T)$ of the 92.5 vol % $Y_{3/4}Lu_{1/4}Ba_2Cu_3O_7$ + 7.5 vol % $Y_3(Al_{1-x}Fe_x)_5O_{12}$ composites [$S + GR$(Fe x)] with iron contents x = 1.0, 0.8, 0.4, 0.3, 0.15, 0.1, and 0.025 in the temperature range T = 4.2–100 K at different transport currents j (indicated in the figures). For all samples, T_{C0} = 93.5 K and T_{C1} = 91.5 K.

Fig. 3h and the inset to Fig. 4a, which show the dependences $R(T)$ at different transport currents (the inset to Fig. 4a shows the dependences $R(T)$ in the immediate vicinity of the temperature T_{C1} on an enlarged scale). It can also be seen from Fig. 4a that the applied magnetic field brings about an increase in the electrical resistance of the composite in both temperature ranges T_{C0}–T_{C1} and $T < T_{C0}$. A strong magnetic field (10, 60 kOe) leads to a smearing of the superconducting transition in high-temperature superconductor crystallites, and this effect is comparable to that observed for single-crystal samples. A similar behavior of the dependences $R(T, j, H)$ is also characteristic of composites with low iron contents, such as $S + GR$(Fe 0.03), $S + GR$(Fe 0.025) (Fig. 3g), $S + GR$(Fe 0.05), and $S + GR$(Fe 0.1) (Fig. 3f).

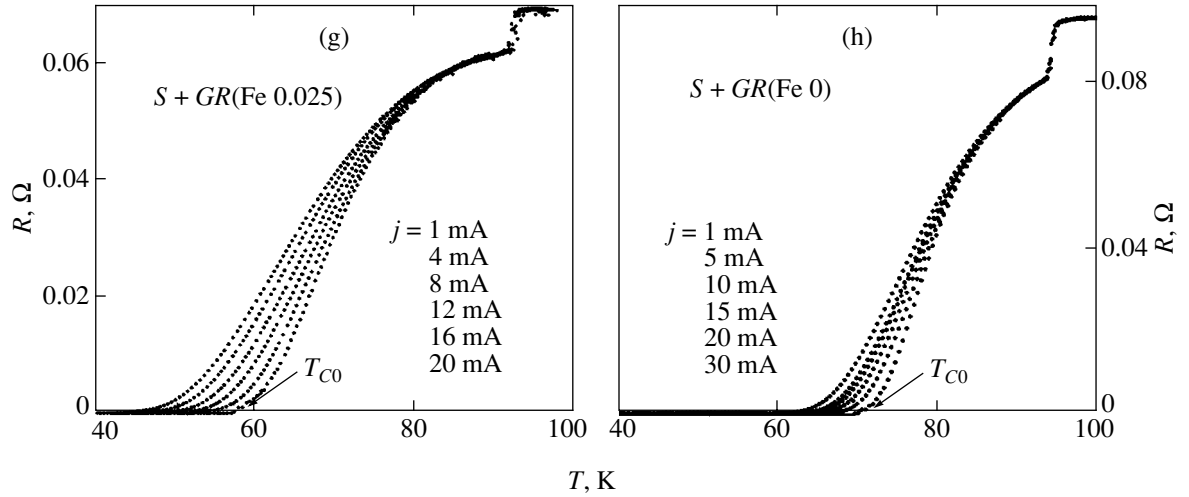

Fig. 3. (Contd.).

A different situation is observed for composites with an iron content $x = 0.15$ and higher. As can be seen from Figs. 3a–3e and 4b, not two but three portions in the ranges T_m–T_{C1}, T_{C0}–T_m, and $T < T_{C0}$ (the corresponding characteristic temperatures are presented in Fig. 4b) can be distinguished in the dependences $R(T)$. In the range from temperature T_{C1} to temperature T_m, the electrical resistance does not depend on the transport current. Moreover, the applied magnetic field (up to several kilooersteds) in this temperature range likewise does not affect the dependence $R(T)$. Only at temperatures below the temperature T_m characteristic of the given composite do the dependences $R(T)$ become functions of the current (Figs. 3a–3e) and the magnetic field strength (Fig. 4b). For all of the composites with magnetoactive components, except for the $S + GR$(Fe 1.0) composite, it is possible to distinguish the third temperature range $T < T_{C0}$. On the whole, the transport properties of the composites in this range are similar to those for the sample with pure aluminum garnet $S + GR$(Fe 0).

It should be noted that the nonlinearity of the current–voltage characteristics (even at $j_C = 0$) and the magnetoresistance are the specific features and integral characteristics of the Josephson effect for both a single junction and a network of junctions. Therefore, the fact that the temperature dependence of the electrical resistance involves a portion in which the electrical resistance depends neither on the transport current nor on the magnetic field strength can be interpreted as complete suppression of the Josephson coupling in the temperature range under consideration. When supercurrent carriers tunnel through magnetoactive interlayers separating high-temperature superconductor grains, Cooper pairs interact with magnetic moments localized in barriers. This interaction tends to destroy a Cooper pair (to align the spins of supercurrent carriers in parallel). The Josephson coupling energy and the exchange energy of

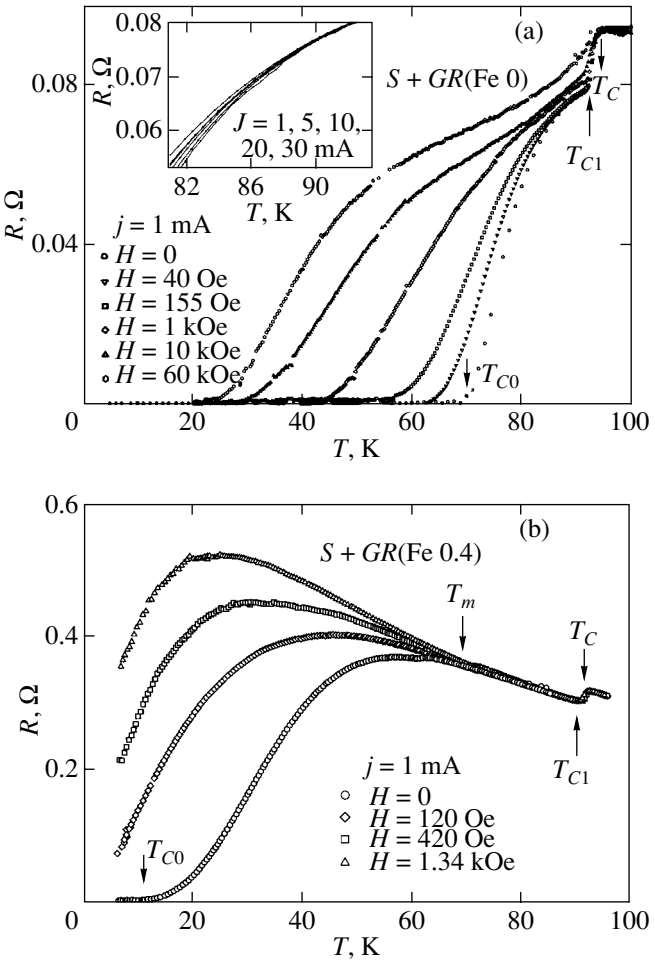

Fig. 4. Temperature dependences of the electrical resistance $R(T)$ of the 92.5 vol % $Y_{3/4}Lu_{1/4}Ba_2Cu_3O_7$ + 7.5 vol % $Y_3(Al_{1-x}Fe_x)_5O_{12}$ composites with iron contents x = (a) 0 and (b) 0.4 in the temperature range T = 4.2–100 K at different strengths of the applied magnetic field.

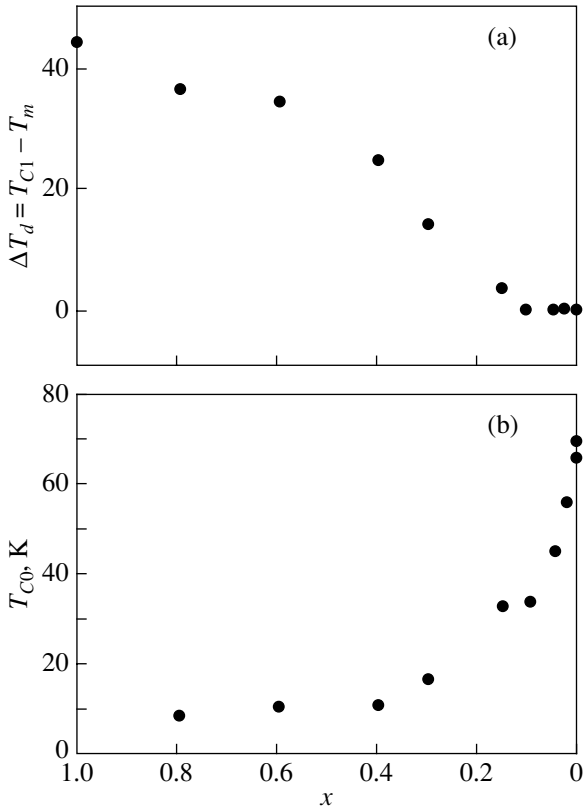

Fig. 5. Dependences of (a) the width of the temperature range $\Delta T_d = T_{C1} - T_m$ (see text and Fig. 4a) and (b) the temperature T_{C0} on the iron content x in the 92.5 vol % $Y_{3/4}Lu_{1/4}Ba_2Cu_3O_7$ + 7.5 vol % $Y_3(Al_{1-x}Fe_x)_5O_{12}$ composites. $T_{C1} = 91.5$ K.

this interaction compete with each other. Kuplevakhskiĭ and Fal'ko [19] theoretically proved that, at a critical thickness d_C of the dielectric barrier (and, naturally, at $d > d_C$), the Josephson coupling between two superconductors disappears; i.e., the energy gap in the barrier region becomes equal to zero because of the scattering of Cooper pairs by the magnetic moments in the barrier. Recall that the Josephson coupling energy is proportional to the energy gap. Therefore, as the temperature decreases, an increasing number of carriers transfer to a superconducting condensate and the Josephson coupling at a specific temperature begins to dominate over the mechanism of destruction of Cooper pairs due to the interaction with magnetic moments. In our opinion, the experimentally observed temperature T_m characteristic of the majority of composites containing iron in the garnet is a critical temperature below which the Josephson coupling energy becomes higher than the energy of the interaction between the magnetic moments of iron ions and Cooper pairs.

The effective geometric thickness d of the barriers depends on the volume concentration of the nonsuperconducting component [23, 25]. In our previous paper [26], we demonstrated that the temperature T_m depends on the volume concentration of the $Y_3Fe_5O_{12}$ component in the composites (i.e., on the effective thickness d) and decreases with an increase in the effective thickness d. It can be seen from Fig. 3 that the temperature T_m shifts toward the high-temperature range as iron is replaced by aluminum in the $Y_3(Al_{1-x}Fe_x)_5O_{12}$ garnet. Therefore, the degree of substitution of aluminum atoms for magnetoactive iron atoms in the $Y_3(Al_{1-x}Fe_x)_5O_{12}$ garnet affects the specific temperature T_m. The temperature T_m decreases with an increase in the iron content x. The dependence of the width of the temperature range $\Delta T_d = T_{C1} - T_m$ on the iron content x in the $Y_3(Al_{1-x}Fe_x)_5O_{12}$ material of barriers between high-temperature superconductor grains is shown in Fig. 5a. At $x = 0.15$, the width of the temperature range is approximately equal to 2 K. The behavior of the dependences $R(T)$ for the composites containing the garnet component with an iron content $x = 0.1$ or lower is similar to that of the dependence $R(T)$ for the composite with the $Y_3Al_5O_{12}$ nonmagnetic component.

In our opinion, a similar effect was observed for single Josephson junctions with ferromagnetic barriers. In the pioneering work by Claeson [41], it was shown that the energy gap in iron barriers in Pb/Fe/Pb junctions is equal to zero at a temperature $T \approx 0.7$ K. Bourgeois et al. [6, 7] studied Nb/Al/Gd/Al/Nb single junctions. The temperature dependences $R(T)$ obtained for these materials also exhibit three portions below the transition temperature of the superconducting boundaries ($T_C \approx 7.6$ K for Nb). According to the notation introduced in the present paper, the characteristic temperatures determined in [6] are as follows: $T_m \approx 5.2$ K and $T_{C0} \approx 3.2$ K at $d_{Gd} = 4$ nm and $T_m \approx 4.0$ K and $T_{C0} \approx 1.1$ K at $d_{Gd} = 8$ nm.

The content of magnetoactive atoms in the nonsuperconducting component also affects the specific quantities that characterize the Josephson coupling strength in the $S + GR$(Fe x) composites. First and foremost, we dwell on the dependence of the temperature T_{C0} on the iron content x at a fixed volume concentration of the garnet in the composite (Fig. 5b). This dependence is monotonic and characterizes the temperature range T_{C0}–T_C in which the critical current in the composite is equal to zero. The influence of the volume concentration of the nonsuperconducting component on this parameter of the composites was studied in our previous work [26]. Now, we consider in greater detail the dependences $R(T, j)$. For the composites with sufficiently strong Josephson coupling (at low iron contents $x = 0$–0.15 in the garnet), an increase in the transport current from 1 to 20–30 mA leads to a shift of the temperature T_{C0} toward the low-temperature range by 10–15 K (Figs. 3e–3h). For the composites with a higher iron content in the garnet, the same shift of the temperature T_{C0} is observed for a smaller change in the transport current j: from 1 to 8 mA for the $S + GR$(Fe 0.3) composite (Fig. 3d) and from 0.1 to 4.0 mA for the $S +$

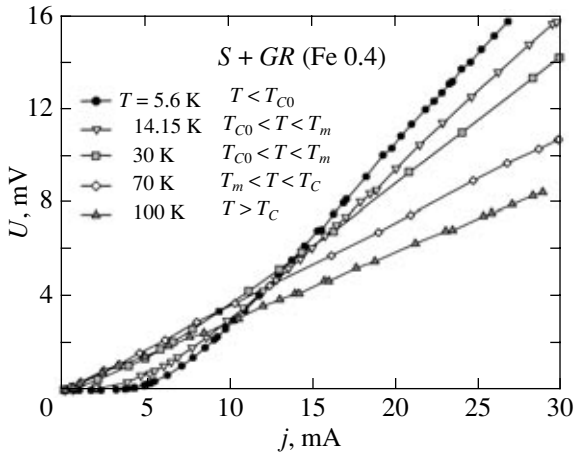

Fig. 6. Current–voltage characteristics for the 92.5 vol % $Y_{3/4}Lu_{1/4}Ba_2Cu_3O_7$ + 7.5 vol % $Y_3(Al_{0.6}Fe_{0.4})_5O_{12}$ composite [*S* + *GR*(Fe 0.4)].

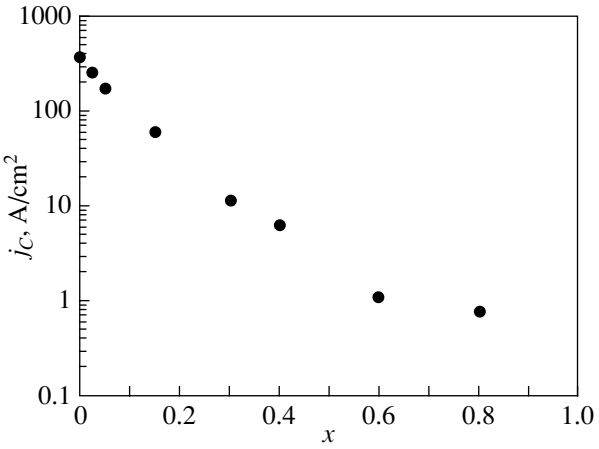

Fig. 7. Dependence of the critical current density j_C on the iron content x in the nonsuperconducting component of the 92.5 vol % $Y_{3/4}Lu_{1/4}Ba_2Cu_3O_7$ + 7.5 vol % $Y_3(Al_{1-x}Fe_x)_5O_{12}$ composites at a temperature of 4.2 K.

GR(Fe 0.4) composite (Fig. 3c). The dependences $R(T)$ measured for the composites at $x = 0.3$ at high transport current densities indicate that electrical resistance does not vanish at all.

At temperatures lower than the temperature T_m, the dependences $R(T)$ obtained for the composites with an iron content $x = 0.15$ exhibit a nonmonotonic behavior (Figs. 3a–3e). As the temperature decreases, the electrical resistance $R(T)$ of these composites increases and reaches a maximum at a particular temperature. The positions of the maxima in the dependences $R(T)$ shift toward the low-temperature range with an increase in the transport current. This behavior results from the competition of two mechanisms, namely, the Josephson tunneling observed in the range below the temperature T_m (at low currents of 0.1–1.0 mA) and conventional single-particle tunneling through dielectric interlayers. It should be noted that the probability of Josephson tunneling decreases as the transport current and magnetic field strength increase. It is evident that an increase in the transport current leads to transformation of the composite sample (i.e., the network of Josephson junctions in the composite) into a resistive state and that the current flow occurs through the single-particle tunneling mechanism. As was noted above, the Josephson tunneling mechanism becomes dominant over the other mechanism with a decrease in the temperature and the resistance of the sample begins to decrease. In other words, the dependence of the electrical resistance for the composite in the resistive state, in which the Josephson coupling is suppressed, exhibits a semiconductor behavior, as is the case in the range above the temperature T_C.

Figure 6 depicts the current–voltage characteristics of the *S* + *GR*(Fe 0.4) composite at different temperatures. These current–voltage characteristics illustrate the resistive state of the composite. At temperatures below the temperature T_{C0}, the current–voltage characteristics involve portions with $U = 0$ (which indicates the presence of the critical current). The nonlinear portion is observed with an increase in the current. At currents of 15–20 mA, the voltage drop depends almost linearly on the current. This means that Josephson links virtually transform into the normal state under the current. It is at these transport currents j that the dependences $R(T)$ obtained for the composites at low temperatures exhibit a semiconductor behavior. This behavior is observed in the range above the temperatures T_C and T_m. At temperatures higher than the temperature T_{C0} (in the range $T_{C0} < T < T_m$), the current–voltage characteristics $U(j)$ emerge from the origin of the coordinates ($j_C = 0$) and, in the initial portion, are nonlinear functions of the current. At temperatures of 70 K ($T > T_m$) and 100 K ($T > T_C$), the current–voltage characteristics are linear functions. For high current densities, the slopes of the current–voltage characteristics $U(j)$ are larger at low temperatures. This confirms the results obtained in the analysis of the temperature dependences of the electrical resistance $R(T)$.

The dependence of the critical current density on the iron content in the nonsuperconducting component of the composites at 4.2 K is plotted in Fig. 7. In the logarithmic coordinates with respect to the critical current density j_C, virtually all points fit a straight line. This suggests that the critical current density j_C is adequately described by an approximately exponential dependence $j_C(x) \sim \exp(-x)$. The exception is provided by the point at $x = 0.8$, because the error in the determination of the critical current density j_C increases at low transport currents. It should be noted that the grain boundaries in the series of composites under investigation have an equal effective thickness because the composites contain the nonsuperconducting component at an identical volume

concentration and the samples were prepared according to the same technology under the same conditions. Therefore, the revealed dependences of the quantities T_m, T_{C0}, and j_C(4.2 K), as well as the behavior of the dependence $R(T)$ on the transport current as a function of the iron content x, are governed only by the content of magnetoactive atoms in the garnet. To the best of our knowledge, the dependence of the critical current density for a Josephson junction on the concentration of magnetoactive atoms embedded in this junction has never been analyzed theoretically. The experimental data obtained in this study can serve as the first step toward understanding the mechanisms of suppression of weak-coupling high-temperature superconductivity by magnetic scattering centers that are embedded in the material of the Josephson junction so that the mean distances ξ between these centers are multiples of the lattice constant of the insulator.

5. CONCLUSIONS

Thus, the transport properties of a network of Josephson junctions based on high-temperature superconductors with magnetoactive atoms embedded in barriers were investigated for the first time. In the $Y_{3/4}Lu_{1/4}Ba_2Cu_3O_7$ + $Y_3(Al_{1-x}Fe_x)_5O_{12}$ composites under investigation, an increase in the iron content in the $Y_3(Al_{1-x}Fe_x)_5O_{12}$ material of barriers separating high-temperature superconductor crystallites leads to a reduction of the Josephson coupling strength due to the destruction of Cooper pairs as a result of the interaction with magnetic moments of iron atoms. For a particular iron content $x \geq 0.15$, the Josephson coupling is completely suppressed in the temperature range $\Delta T_d = T_m - T_{C1}$, and this range increases with an increase in the iron content x.

ACKNOWLEDGMENTS

We would like to thank A.F. Bovina for performing the x-ray diffraction analysis, A.D. Balaev for his participation in discussions of the results obtained in this study, O.A. Bayukov for performing Mössbauer investigations, and V. Knapf for assistance in performing the experiments. D.A. Balaev acknowledges Yu.N. Proshin and J. Cayssol for their participation in discussions of the results and for helpful remarks.

This work was supported by the Russian Foundation for Basic Research (project no. 04-02-16710a) and the Council on Grants from the President of the Russian Federation for the Support of Young Candidates of Science and Leading Scientific Schools of the Russian Federation (project no. MK-3781.2004.2).

REFERENCES

1. A. S. Borukhovich, Usp. Fiz. Nauk **169** (7), 737 (1999) [Phys. Usp. **42** (7), 653 (1999)].
2. A. Yu. Izyumov, Yu. N. Proshin, and M. G. Khusainov, Usp. Fiz. Nauk **172** (2), 113 (2002) [Phys. Usp. **45** (2), 109 (2002)].
3. Y. Tanaka and S. Kashivaya, J. Phys. Soc. Jpn. **69**, 1152 (2000).
4. M. Fogelstrom, Phys. Rev. B: Condens. Matter **62**, 11812 (2000).
5. J. Cayssol and G. Montambaux, Phys. Rev. B: Condens. Matter **71**, 012507 (2005).
6. O. Bourgeois, P. Gandit, A. Sulpice, J. Chaussy, J. Lesueur, and X. Grison, Phys. Rev. B: Condens. Matter **63**, 064517 (2002).
7. O. Bourgeois, P. Gandit, J. Lesueur, A. Sulpice, X. Grison, and J. Chaussy, Eur. Phys. J. B **21**, 75 (2001).
8. M. D. Lawrence and N. Giordano, J. Phys.: Condens. Matter **11**, 1089 (1999).
9. M. Schock, C. Surgers, and H. V. Lohneysen, Eur. Phys. J. B **14**, 1 (2000).
10. V. V. Ryazanov, V. A. Oboznov, A. Yu. Rusanov, A. V. Veretennikov, A. A. Golubov, and A. A. Aarts, Phys. Rev. Lett. **86**, 2427 (2001).
11. S. M. Frolov, D. J. van Harlingen, V. A. Oboznov, V. V. Bolginov, and V. V. Ryazanov, Phys. Rev. B: Condens. Matter **70**, 144505 (2004).
12. C. Bell, R. Lotoee, G. Burnell, and M. G. Blamire, Phys. Rev. B: Condens. Matter **71**, 180501 (2005).
13. Ondrey Vavra, S. Gazi, I. Vavra, J. Derer, and E. Kovacova, Physica C (Amsterdam) **404**, 395 (2004).
14. V. M. Krasnov, O. Erisson, S. Intiso, P. Delsing, V. A. Oboznov, A. S. Prokofiev, and V. V. Ryazanov, Physica C (Amsterdam) **418**, 16 (2005).
15. H.-U. Habermeier, J. Albrecht, and S. Soltan, Supercond. Sci. Technol. **17**, 140 (2004).
16. Kun Zhao, Y. H. Huang, J. F. Feng, Li Zhang, and H. K. Wong, Physica C (Amsterdam) **418**, 138 (2005).
17. L. N. Bulaevskiĭ, V. V. Kuziĭ, and A. A. Sobyanin, Pis'ma Zh. Éksp. Teor. Fiz. **25** (7), 314 (1977) [JETP Lett. **25** (7), 290 (1977)].
18. L. N. Bulaevskii, V. V. Kuzii, and S. V. Panyukov, Solid State Commun. **44**, 539 (1982).
19. S. V. Kuplevakhskiĭ and I. I. Fal'ko, Fiz. Nizk. Temp. (Kharkov) **10** (7), 691 (1984) [Sov. J. Low Temp. Phys. **10** (7), 361 (1984)].
20. S. V. Kuplevakhskiĭ and I. I. Fal'ko, Fiz. Met. Metalloved. **62**, 13 (1986).
21. J. Neimeyer and G. von Minngerode, Z. Phys. B: Condens. Matter Quanta **36**, 57 (1979).
22. V. Pena, Z. Sefrioui, D. Arias, C. Leon, and J. Santamaria, Phys. Rev. Lett. **94**, 057002 (2005).
23. C. Gaffney, H. Petersen, and R. Bednar, Phys. Rev. B: Condens. Matter **48**, 3388 (1993).
24. M. I. Petrov, D. A. Balaev, K. A. Shaĭkhutdinov, and K. S. Aleksandrov, Fiz. Tverd. Tela (St. Petersburg) **41** (6), 969 (1999) [Phys. Solid State **41** (6), 881 (1999)].
25. M. I. Petrov, D. A. Balaev, K. A. Shaihutdinov, and K. S. Aleksandrov, Supercond. Sci. Technol. **14**, 798 (2001).
26. K. A. Shaĭkhutdinov, D. A. Balaev, S. I. Popkov, and M. I. Petrov, Fiz. Tverd. Tela (St. Petersburg) **45** (10), 1776 (2003) [Phys. Solid State **45** (10), 1866 (2003)].

27. H. S. Gamchi, G. J. Russel, and K. N. R. Taylor, Phys. Rev. B: Condens. Matter **50**, 12950 (1994).

28. M. I. Petrov, D. A. Balaev, K. A. Shaĭkhutdinov, and S. G. Ovchinnikov, Fiz. Tverd. Tela (St. Petersburg) **40** (9), 1599 (1998) [Phys. Solid State **40** (9), 1451 (1998)].

29. M. I. Petrov, D. A. Balaev, K. A. Shaĭkhutdinov, and S. I. Popkov, Pis'ma Zh. Éksp. Teor. Fiz. **75** (3), 166 (2002) [JETP Lett. **75** (3), 138 (2002)].

30. A. D. Balaev, Yu. V. Boyarshinov, M. M. Karpenko, and B. P. Khrustalev, Prib. Tekh. Éksp., No. 3, 167 (1985); Available form VINITI, No. 69-85.

31. A. Barone and G. Paterno, *Physics and Applications of the Josephson Effect* (Wiley, New York, 1982; Mir, Moscow, 1982).

32. S. Geller, H. J. Williams, G. P. Espinosa, and R. C. Sherwood, Bell Syst. Tech. J. **43**, 565 (1964).

33. M. A. Gilleo and S. Geller, Phys. Rev. **10**, 1 (1958).

34. F. Grasset, S. Mornet, A. Demourgues, J. Portier, J. Bonnet, A. Vekris, and E. Duguet, J. Magn. Magn. Mater. **234**, 409 (2001).

35. Ch. S. Kim, B. Ki. Min, S. J. Kim, S. R. Yoon, and Y. R. Uhm, J. Magn. Magn. Mater. **254–255**, 553 (2003).

36. S. Thongmee, P. Winotai, and I. M. Tang, Solid State Commun. **109**, 471 (1999).

37. C. Y. Chen, G. J. Pogatshnik, Y. Chen, and M. R. Kokta, Phys. Rev. B: Condens. Matter **38**, 13 (1988).

38. S. R. Rotman, Phys. Rev. B: Condens. Matter **41**, 791 (1990).

39. S. Krupička, *Physik der Ferrite und der verwandten magnetischen Oxide* (Academia, Prague, 1973; Mir, Moscow, 1976), Vol. 1.

40. V. Ambegaokar and B. I. Halperin, Phys. Rev. Lett. **22**, 1364 (1969).

41. T. Claeson, Thin Solid Films **66**, 151 (1980).

Translated by O. Borovik-Romanova